

B7 Homolog 6 Promotes the Killing Activity of Natural Killer Cells Against Cervical Cancer Through the Downstream ERK Pathway of Nkp30

Ruimeng Guo¹, Ou Chai¹, Changying Li^{2*}, Yanying Xu³, XueWang Guo³ and Fang Wang³

¹Department of Gynecology, The second hospital of Tianjin Medical University, Tianjin. P.R.China

¹Department of Obstetrics and Gynecology, Chu Hsien-I Memorial Hospital, Tianjin. P.R.China

²Department of Tianjin Institute of Urology, The second hospital of Tianjin Medical University, Tianjin. P.R.China

³Department of Gynecology, The second hospital of Tianjin Medical University, Tianjin. P.R.China

*Corresponding Author:

Changying Li, Department of Tianjin Institute of Urology, The second hospital of Tianjin Medical University, Tianjin. P.R.China

Received: 08 Mar 2025

Accepted: 15 Mar 2025

Published: 20 Mar 2025

J Short Name: J CMI

Copyright: ©2025 C Li, This is an open access article distributed under the terms of the Creative Commons Attribution License, which permits unrestricted use, distribution, and build upon your work non-commercially.

Keywords: B7 Homolog 6; Cervical Cancer; HeLa Cells; Immune Regulation; NKp30; ERK Pathway

Citation: C Li. B7 Homolog 6 Promotes the Killing Activity of Natural Killer Cells Against Cervical Cancer Through the Downstream ERK Pathway of Nkp30. *J Clin Med Img.* 2025; V8 (7): 1-7

1. Abstract

As a ligand of NKp30, B7 homolog 6 (B7-H6) is involved in the immune regulation of various tumors. The aim of the present study was to clarify the effect of B7-H6 expression in HeLa cells on the killing function of natural killer (NK) cell. B7 H6 expression was changed in HeLa cells using short hairpin RNA. The effect of B7-H6 on the killing function of NK cells was analyzed following cell co-culture. Flow cytometry was used to detect NKp30 expression, degranulation function, and perforin (PFP) and granzyme B (GZMB) secretion function of NK cells. Enzyme-linked immunosorbent assay was used to detect interferon- γ (INF- γ) production. The cytotoxicity of NK-92 cells was determined using the CytoTox 96[®] Non-Radioactive Cytotoxicity Assay. Western blotting was used to detect the ERK phosphorylation level in NK cells. Following the co-culture of NK-92 and HeLa cells with different B7-H6 expression levels, the NKp30 expression, NK-92 cell killing rate, PFP and INF- γ production, as well as degranulation function, were changed in NK cells; no effect on GZMB production was observed. Following cell co-culture, the ERK phosphorylation level in NK cells was gradually increased with the upregulation of B7-H6. B7-H6 may enhance the killing capacity of NK cells by activating the NKp30 downstream ERK signaling pathway.

2. Introduction

Imbalanced immune regulation plays an important role in the occurrence and development of tumors. In order to develop, tumors must successfully evade innate immunity. There are a large number of studies about immune regulation of cervical cancer, involving T cells, dendritic cells, macrophages, neutrophils and inflammatory factors [1]. And Pembrolizumab, which has limited clinical effect, has been approved as a programmed death-1 (PD-1)/ PD ligand 1 immune target blocker for second-line treatment of cervical cancer. But the involvement of innate immunity in the immune regulation mechanism and immune target drugs of cervical cancer is rarely reported. NK cells are the main effector cells of the innate immune system. A decrease in the NK cell killing activity in cervical cancer is one of the causes of immune escape [1]. Natural cytotoxic receptors (NCRs) are the main activated receptors of NK cells, and NKp30 is a primary immunoglobulin in the NCR receptor family [3]. B7-H6, an NKp30 ligand, is expressed on the surface of some tumor cells but not on normal cells [4-7]. Textor et al.[8]. Found that, in a variety of tumor cells, including SK-Mel-37, A375, Capan-1 and Raji cells, B7-H6 knockdown can reduce the expression of NKp30 and affect the degranulation function of NK cells. Our preliminary study found that B7-H6 is differentially expressed in cervical lesions, promotes the progression of cervical cancer [9] and is associated with clinical parameters of cervical cancer [10]. In the present study, the effect of B7-H6 expression on the surface of HeLa cells on NK cell killing function was explored through NKp30.

3. Materials and Methods

Cell lines. A HeLa human cervical cancer cell line was obtained from the General Hospital of Tianjin Medical University (Tianjin, China). The HeLa cells were cultured into RPMI 1640 medium (cat. no. 31870074; Invitrogen; Thermo Fisher Scientific, Inc.) supplemented with 10% FBS (cat. no. F8318; Sigma Aldrich; Merck KGaA), and maintained at 37°C in a humidified atmosphere containing 5% CO₂. The NK-92 cell line was purchased from BNCC Biotechnology Co. Ltd. The cells were cultured in vitro in special culture medium for NK-92 cells (cat. no. 5293/50; R&D Systems, Inc.), consisting of MEM α , 0.2 mM inositol, 0.1 mM β -mercaptoethanol, 0.02 mM folic acid, 2.5% FBS, supplemented with recombinant human IL-2 (cat. no. 5293/50; R&D Systems, Inc.) at a ratio of 1:500, 1X L-glutamine (Invitrogen; Thermo Fisher Scientific, Inc.) and antibiotics (penicillin/streptomycin; Invitrogen; Thermo Fisher Scientific, Inc.). The NK-92 cells were maintained at 37°C in a humidified atmosphere containing 5% CO₂. **Cell co-culture.** The HeLa cells in each group were inoculated into 6-well plates at a density of 2x10⁵ cells/well, and 1 ml RPMI 1640 complete medium was added. Each 6-well plate was labeled, and the cell density and growing status were observed under the microscope (Olympus Corporation). The cells were placed in an environment containing 5% CO₂ at 37°C for 6h. Once HeLa cells had adhered to the wall, the cell culture medium was removed, and the NK-92 cells with the best growth condition were selected for culture in 6-well plates at a density of 1x10⁶ cells/well, according to the ratio of NK-92 cells (effector cells) and HeLa cells (target cells) (E:T = 5:1). Special culture medium for NK-92 cells (2 ml) containing IL-2 was added to each well and cultured at 37°C with 5% CO₂ for 4 h. Short hairpin RNA (shRNA) transfection. The shRNA sequence of 28 μ g/ml interfering with B7-H6 (shB7-H6) and a control shRNA sequence (shNC) were synthesized by Suzhou GenePharma Co., Ltd. In addition, overexpressed B7-H6 gene sequence (hB7-H6) and control sequence (hNC) were obtained from Suzhou GenePharma Co., Ltd., according to the full length of CoDing Sequence region of the human B7-H6 gene. Sequence details are shown in Table S1. The pGLV3/H1/GFP lentiviral vectors (LV) LV3 shRNA or LV3 shRNA NC [multiplicity of infection (MOI), 10], and the EF-1 α /GFP&Puro LVs, LV5-hB7-H6 or LV5-hNC (MOI, 10), were transfected into HeLa cells at 37°C, and screened with polybrene (1.5 μ g/ml; dilution, 1:1,000; Suzhou GenePharma Co., Ltd.). Viral infections were performed serially. A fluorescence microscope (Olympus Corporation) was used to observe whether fluorescence transfection efficiency was >80% after 48 h of transfection. Stable cell lines expressing gene sequences were selected using 2 μ g/ml puromycin 72 h after transfection. Reverse transcription quantitative PCR (RT qPCR). Total RNA was extracted from cultured cells using TRIzol[®] reagent (cat. no. 213407; Invitrogen; Thermo Fisher Scientific, Inc.). Purified RNA was then reverse-transcribed to cDNA using RevertAid First Strand cDNA Synthesis Kit purchased from Thermo Fisher Scientific, Inc. Next, RT-qPCR was performed using FastStart Universal

Table S1: Sequence Details.

Experiment Name	Gene Name	Cat. No.	Gene Sequence (5'-3')
shB7-H6-1	shRNA-1	190331CZ	CCCTGCTCTCCTAACAGTT
shB7-H6-2	shRNA-2	190331DZ	GGTTCTACCCAGAGGCTAT
shNC	shRNA-NC	C03DZ	TTCTCCGAACGTGTACGT
hB7-H6	NCR3LG1-homo	D02001	The full length of CDS region
hNC	no-load	D03007	—

SYBR Green Master Mix (cat. no. 04913850001; Roche Diagnostics), following the manufacturer's instructions. An initial amplification with denaturation, primer annealing and primer extension was performed using B7-H6 specific primers (5' TTTCCATTCATTGGTGGCCTA 3' forward and 5' TTTCCATTCATTGGTGGCCTA 3' reverse). Data were normalized to the geometric mean of the housekeeping gene GAPDH (5' CTGGAACGGTGAAGGTGACA 3' forward and 5' AAGGGACTTCCTGTAACA ATGCA 3' reverse) to control the variability in expression levels. Western blotting (WB). The HeLa cells were lysed using RIPA lysis buffer (cat. no. BL504A; Biosharp; http://www.biosharp.cn/index/product/details/language/en/product_id/1783.html), and the protein concentration was determined using the Quick Start Bradford protein assay (Bio Rad Laboratories, Inc.). The NK-92 cell lysate consisted of 1 ml RIPA lysis buffer, 10 µl phenylmethylsulfonyl fluoride (cat. no. ST505; Beyotime Biotechnology, Inc.) and 10 µl phosphatase (cat. no. P1048; Beyotime Biotechnology, Inc.) inhibitor. Equal amounts of protein (30 µg loaded per lane) were separated using 10% SDS PAGE and transferred onto PVDF membranes (cat. no. P2938 1ROL; Sigma Aldrich; Merck KGaA). The membranes were blocked at room temperature for 1 h with TBS 0.05% Tween 20 containing 5% skimmed milk powder (HeLa cells) or 5% BSA (NK-92 cells). The membranes of HeLa cell were subsequently incubated with an anti B7 H6 rabbit antibody (cat. no. ab121794; dilution, 1:1,000; Abcam) or an anti GAPDH antibody (cat. no. G8795; dilution, 1:5,000; Sigma Aldrich; Merck KGaA) at 4°C overnight. The membranes of NK-92 cells were subsequently incubated with an anti p44/42 ERK1/2 rabbit antibody (cat. no. 4695T; dilution, 1:5,000; Cell Signaling Technology, Inc.), anti p44/42 p-ERK1/2 rabbit antibody (Thr202/Tyr204; cat. no. 4370T; dilution, 1:5,000; Cell Signaling Technology, Inc.) or an anti GAPDH antibody (cat. no. G8795; dilution, 1:5,000; Sigma Aldrich; Merck KGaA) at 4°C overnight. Following primary antibody incubation, the membranes were incubated with a HRP conjugated goat anti rabbit antibody (cat. no. abs20040; dilution, 1:5,000; Absin Bioscience, Inc.) or goat anti mouse secondary antibody (cat. no. abs20039; dilution, 1:4,000; Absin Bioscience, Inc.) at 37°C for 1 h. Protein bands were visualized using ECL reagent (cat. no. abs920; Absin Bioscience, Inc.). ImageJ software (version no. v1.8.0; National Institutes of Health) was used to quantify the WB data. Flow cytometry. Following co-culture, the NK-92 cells suspended in the culture medium were sucked out, and the NK-92 cells that had not been co-cultured were placed into labeled centrifugal tubes by group and centrifuged at 1,000 x g for 3 min, and the supernatant was discarded. The cells were washed twice with PBS. One part of each group of NK-92 cell samples was used for NK-92 cell membrane staining, and the other part was used for the staining of the encapsulated protein. Fluorescence labeling of cell membrane antigen. The antibodies CD3-APC (5µL/Test, cat. no. 47-0037-42; eBioscience; Thermo Fisher Scientific, Inc.), CD56-FITC (5µL/Test, cat. no. 304603; BioLegend, Inc.), NKp30-PE/Cy7 (5µL/Test, cat. no. 25-4714-80; eBioscience; Thermo Fisher Scientific, Inc.) and CD107A-PE (5µL/Test, cat. no. 328607; BioLegend, Inc.) were added, fully mixed and incubated for 30 min at room temperature under dark conditions. The cultured cells were washed with PBS and fixed with 4% paraformaldehyde fixative for machine detection and analysis. A single standard control was set for each sample. Fluorescence labeling of intracellular antigen. First, DAPI was added and fully mixed, and cells were then incubated for 20 min at room temperature under dark conditions. The supernatant was then washed twice with PBS and centrifuged at 1,500 x g for 5 min to remove it. A total of 200 µl 4% paraformaldehyde fixative was mixed thoroughly and kept away from light for 30 min at room temperature, followed by washing with PBS twice, centrifugation at 1,500 x g for 5 min, and the removal of the supernatant. Next, 200 µl breaking solution was added, centrifuged at 1,500 x g for 5 min, followed by re-suspension of the cells with 100 µl

breaking solution. Antibodies granzyme B (GZMB)-PE (cat. no. 372208; BioLegend, Inc.) and perforin (PFPE)-eFluor 450 (cat. no. 48-9994-42; eBioscience; Thermo Fisher Scientific, Inc.) were added to the suspended cells and fully mixed, and the cells were incubated at room temperature under dark conditions for 30 min. The incubated cells were washed with PBS, and suspended in 300 µl PBS for machine detection and analysis. Flow cytometry procedure. A NovoCyte D3000 flow cytometer was used to detect stained cells. Data analysis was performed by NovoExpress software (version 1.5; ACEA Biosciences, Inc.). NK cells were gated by CD3+ and CD56+. Cytotoxicity assays. NK-92 cells were co-cultured with HeLa cells, as described above, using different target ratios: 5:1, 10:1 and 20:1. The cytotoxicity of NK-92 cells was determined using the CytoTox 96 Non-Radio Active Cytotoxicity Assay (cat. no. G1780; Promega Corporation), according to the manufacturer's instructions. Enzyme-linked immunosorbent assay (ELISA). The interferon-γ (INF-γ) release ability of NK-92 cells was determined by ELISA. Each reagent was diluted to working concentrations according to the manufacturer's instructions (cat. no. PDIF50C; R&D Systems, Inc.). NK-92 cells were centrifuged at 3,000 x g for 3 min, and no cell supernatant was collected. A total of 100 µl trapping antibody was then added to each well of the 96-well plate, the plate was sealed, and incubation was performed overnight at room temperature. NK-92 cells were centrifuged at 3,000 x g for 3 min, and no cell supernatant was collected. A total of 300 µl of reagent dilution was added to each well, followed by incubation for 1 h at room temperature. The sample well, standard well and blank well were set. Each well is provided with three multiple wells. A total of 100 µl sample was added to the sample well, 100 µl INF-γ standard was added to the standard well and 100 µl reagent diluent was added to the blank well. The well plates were incubated at room temperature for 2 h. A total of 100 µl INF-γ antibody was added to each well, followed by incubation for 2 h at room temperature. A total of 100 µl streptavidin-HRP was added to each well, followed by incubation at room temperature away from light for 20 min. A total of 100 µl 3,3',5,5'-tetramethylbenzidine substrate solution was added to each well, followed by incubation at room temperature, away from light for 20 min. A total of 150 µl stop solution was added to each well to stop the reaction. The solution in each well was mixed until the color changed from blue to yellow. The optical density (OD) value of each well was measured at 450 nm. Calibration was performed by subtracting the OD value of each standard and sample from the blank well. The standard concentration was the abscissa and the OD value was the ordinate. The ELISACalc software (ELISACalc Software, Inc.) was used to calculate the corresponding concentration of the sample according to the OD value of the sample.

3.1. Statistical Analysis

The experimental data were processed using SPSS 22.0 statistical software (IBM, Corp.). GraphPad Prism 8 (GraphPad Software, Inc.) was used to draw graphs and verify results. The data are presented as the mean ± standard deviation (mean ± SD). One-way ANOVA and Bonferonni test were used for comparisons between multiple groups. Comparisons between two groups was performed using independent unpaired samples t-test. P<0.05 was considered to indicate a statistically significant difference. All experiments were repeated three times, and the mean value of experimental results was taken.

4. Results

Knockdown or overexpression of B7-H6 in HeLa cells. Fluorescence microscopy was performed to determine GFP expression, and it showed that the infection efficiency of shB7-H6, shNC, hB7-H6 and hNC to HeLa cells were both >80% (Fig. S1A). RT qPCR was used to analyze the mRNA expression of B7-H6 in HeLa cells. As compared with the shNC

results of 1.31 ± 0.04 , the B7-H6 mRNA level of shB7-H6 was 0.24 ± 0.02 (81% lower; $P < 0.0001$; Fig. S1B). The mRNA level of B7-H6 in hB7-H6 was 1.35 ± 0.21 and that in hNC was 0.84 ± 0.15 . As compared with the hNC, the mRNA level of B7-H6 in hB7-H6 was increased by 61% ($P < 0.05$; Fig. S1D). WB was used to analyze the expression of B7-H6 protein in HeLa cells. As compared with the shNC result of $81,934 \pm 1,848$, the protein expression of B7-H6 in shB7-H6 was $30,541 \pm 4,374$ (63% lower; $P < 0.0001$; Figure S1C). As compared with the hNC ($55,012 \pm 3,130$), the protein expression level of B7-H6 in hB7-H6 was $98,797 \pm 6,382$ (80% higher; $P < 0.01$; Figure 1E). Effect of B7-H6 knockdown on NKp30 expression and NK cell killing function. The rate of NK-92+ cells expressing NKp30 was analyzed by flow cytometry (Figure S2A). The results of NK-92 alone, NK-92+shB7-H6 and NK-92+shNC groups were 0.41 ± 0.24 , 0.61 ± 0.15 and $1.64 \pm 0.57\%$, respectively. Following NK-92+shB7-H6 co-culture, the proportion of NK cells expressing NKp30 was slightly increased compared with the NK-92 alone group, but the difference was not statistically significant. Following co-culture of NK-92+shNC, the proportion of NK-92 cells expressing NKp30 was significantly increased compared with that following culture with NK-92 alone and co-culture with NK-92+shB7-H6 (both $P < 0.05$; Fig. S2B). The expression of CD107a on the surface of NK-92 cells was detected and analyzed to determine the decapitation ability of NK-92 cells. By flow cytometry (Fig. S2A), the positive cell rate of CD107a was detected in every group. The results in the NK-92 alone, NK-92+shB7-H6 and NK-92+shNC groups were 32.36 ± 2.11 , 40.07 ± 3.60 and $64.72 \pm 3.96\%$, respectively. Compared with the NK-92 alone group, the NK-92+shB7-H6 group exhibited a slight increase in CD107a expression, with no statistically significant difference. The rate of CD107a+ cells in the NK-92+shNC group was significantly increased compared with that in the NK-92 alone $P < 0.0001$ and NK-92+shB7-H6 $P < 0.001$ groups (Figure S2C). The effect of B7-H6 on GZMB secretion in NK-92 cells was analyzed by intracellular staining. The flow cytometry detected the positive cell rate of GZMB in each group (Figure S2A). The results in NK-92 alone, NK-92+shB7-H6 and NK-92+shNC groups were 95.47 ± 3.84 , 92.77 ± 3.03 and $93.57 \pm 3.30\%$, respectively. No statistically significant difference was observed in the GZMB secretion capacity of

NK-92 cells (Figure S2D). The effect of B7-H6 on PFP secretion in NK-92 cells was analyzed by intracellular staining. The flow cytometry detected the positive cell rate of PFP in each group (Figure S2A). The results in the NK-92 alone, NK-92+shB7-H6 and NK-92+shNC groups were 8.96 ± 0.61 , 2.76 ± 1.37 and $4.89 \pm 3.16\%$, respectively. Compared with NK-92 alone, the rate of NK-92 cells secreting PFP in the NK-92+shB7-H6 and NK-92+shNC groups was significantly decreased (both $P < 0.0001$). However, when NK-92+shB7-H6 was compared with NK-92+shNC, the rate of NK-92 cells secreting PFP showed a trend corresponding to that of B7-H6. When NK-92+shNC was compared with the NK-92+shB7-H6, the rate of NK-92 cells secreting PFP in NK-92+shNC was increased ($P < 0.01$; Figure S2E). The effect of B7-H6 on INF- γ secretion in NK-92 cells was analyzed using ELISA in each group (Figure S2F). The results of NK-92 alone, NK-92+shB7-H6 and NK-92+shNC were $4,186.67 \pm 189.03$ pg/ml, $4,402.67 \pm 149.14$ pg/ml and $5,883.83 \pm 433.56$ pg/ml, respectively. No statistically significant difference was observed between the NK-92 alone and NK-92+shB7-H6. Compared with the NK-92+shNC group, the concentration of INF- γ secreted in the NK-92 alone and NK-92+shB7-H6 groups was significantly decreased (both $P < 0.01$). NK-92 cells were co-cultured with each group of HeLa cells according to the different E:T ratios (5:1, 10:1 and 20:1), and then the killing rate of NK-92 cells was detected (Figure S2G). Following co-culture at an E:T of 5:1, the killing rates were $11.37 \pm 1.07\%$ (NK-92+shB7-H6) and $18.00 \pm 2.11\%$ (NK-92+shNC). Following co-culture according to 10:1, the killing rates were $19.00 \pm 2.00\%$ (NK-92+shB7-H6) and $32.00 \pm 4.58\%$ (NK-92+shNC). Following co-culture at an E:T of 20:1, the killing rates were $38.67 \pm 1.53\%$ (NK-92+shB7-H6) and $32.71 \pm 3.22\%$ (NK-92+shNC). Compared with the NK-92+shNC group, the killing rate of NK-92 cells in the NK-92+shB7-H6 group was reduced at both 5:1 ($P < 0.01$) and 10:1 ($P < 0.001$). When the E:T was 20:1, in the NK-92+shB7-H6 group, no statistical difference was observed compared with the NK-92+shNC. Effect of B7-H6 upregulation on NKp30 expression and NK cell killing function. The positive cell rate of NK-92 cells expressing NKp30 was analyzed by flow cytometry (Figure S3A). The results in the NK-92 alone, NK-92+hB7-H6 and NK-92+hNC groups were 0.41 ± 0.24 , 3.81 ± 0.28 and $2.21 \pm 0.25\%$, respectively. As

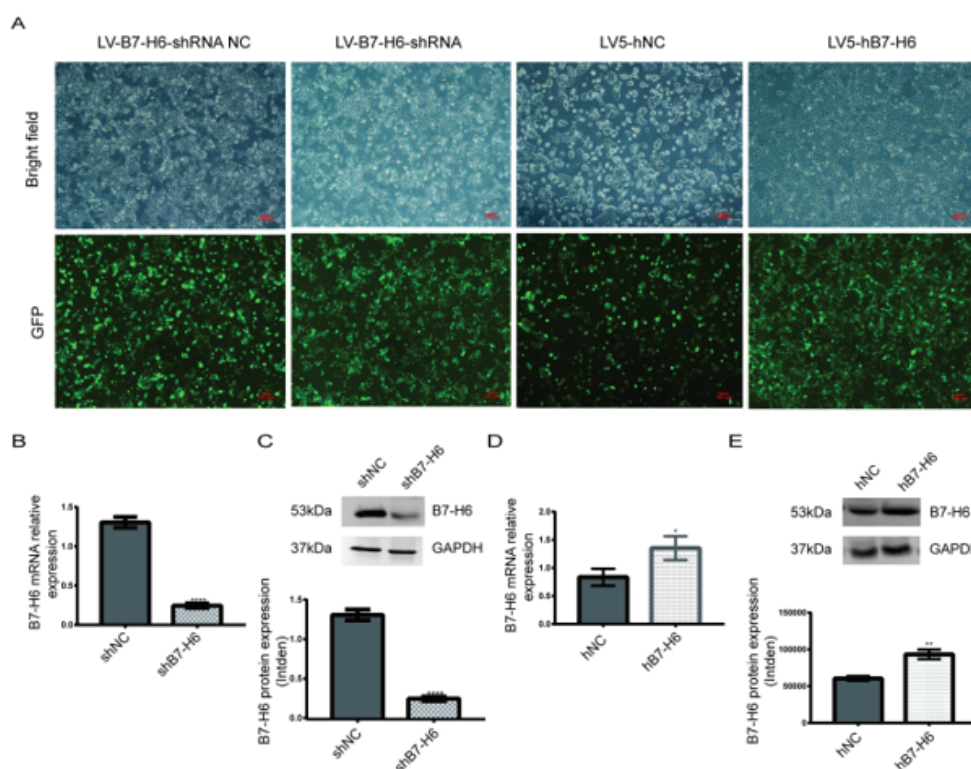


Figure S1: Verification of HeLa cell transfection. (A) Fluorescence microscopy was used to analyze GFP expression in HeLa cells. Magnification, x100; scale, 100 μ m. (B) Compared with shNC, the mRNA level of shB7-H6 was decreased. (C) Compared with shNC, the protein expression level of shB7-H6 was decreased. (D) Compared with hNC, the mRNA level of B7-H6 in hB7-H6 was increased. (E) Compared with hNC, the B7-H6 protein expression level in hB7-H6 was significantly increased.

compared with the NK-92+hNC groups, NK-92 cells expressing NKp30 in the NK-92+hB7-H6 group were significantly upregulated ($P<0.001$). In the NK-92 alone group, the percentage of NKp30+ cells was significantly lower than that in the NK-92+hNC group ($P<0.001$; Figure S3B). The positive cell rate of CD107a in each group was detected using flow cytometry. The results in the NK-92 alone, NK-92+hB7-H6 and NK-92+hNC groups were 32.36 ± 2.11 , 73.31 ± 3.83 and $63.18\pm 3.55\%$, respectively. Compared with the NK-92+hNC group, the percentage of CD107a-expressing cells in the NK-92+hB7-H6 group increased ($P<0.05$). In the NK-92 alone group, the percentage of CD107a-expressing cells was significantly decreased compared with that in the NK-92+hNC group ($P<0.0001$; Figure S3C). The positive cell rate of NK-92 cells secreting GZMB was detected in each group using flow cytometry (Figure S3A). The results in the NK-92 alone, NK-92+hB7-H6 and NK-92+hNC groups were 95.47 ± 3.84 , 94.30 ± 3.65 and $95.90\pm 2.27\%$ respectively. No statistically significant differences were observed (Figure S3D). The positive cell rate of NK-92 cells secreting PFP was detected in each group using flow cytometry. The results in the NK-92 alone, NK-92+hB7-H6 and NK-92+hNC groups were 8.96 ± 0.61 , 2.23 ± 0.30 and $1.01\pm 0.36\%$ respectively. The positive cell rate in the NK-92+hB7-H6 and NK-92+hNC groups were both significantly decreased compared with that in the NK-92 alone group ($P<0.0001$). However, when NK-92+hB7-H6 compared with the NK-92+hNC group, the positive cell rate in NK-92+hB7-H6 was more higher ($P<0.05$; Figure S3E). The concentration of INF- γ secreted by NK-92 cells was detected in each group using ELISA. The results in the NK-92 alone, NK-92+hB7-H6 and NK-92+hNC groups were $4,186.67\pm 189.03$ pg/ml, $6,511.00\pm 234.72$ pg/ml and $5,494.33\pm 224.26$ pg/ml respectively. Compared with NK-92 alone, INF- γ concentration in the NK-92+hNC ($P<0.001$) and NK-92+hB7-H6 ($P<0.0001$) groups was significantly increased. INF- γ concentration in the NK-92+hB7-H6 group was significantly higher than that in the NK-92+hNC group ($P<0.01$; Figure S3F). The killing rate of NK-92 cells was

then detected (Figure S3G). Following co-culture according to a 5:1 E:T, the killing rates of NK-92 cells were $32.83\pm 2.65\%$ (NK-92+hB7-H6) and $19.34\pm 2.08\%$ (NK-92+hNC). Following co-culture according to 10:1 E:T, the killing rates of NK-92 cells were $42.19\pm 2.89\%$ (NK-92+hB7-H6) and $29.30\pm 4.73\%$ (NK-92+hNC). Following co-culture according to 20:1 E:T, the killing rates of NK-92 cells were $50.02\pm 1.99\%$ (NK-92+hB7-H6) and $43.12\pm 2.52\%$ (NK-92+hNC). At 5:1 and 10:1, compared with the NK-92+hB7-H6, the cell killing rate of NK-92 in the NK-92+hNC group was decreased (both $P<0.001$). Finally, at 20:1, the killing rate of NK-92 cells in the NK-92+hNC group was also reduced, as compared with that in NK-92+hB7-H6 ($P<0.05$). Effect of B7-H6 on ERK pathway in NK-92 cells. According to the results of the above co-culture experiment, the NK-92 alone, NK-92+hNC and NK-92+hB7-H6 groups, which exhibited a significant change in NKp30 expression and NK-92 cell killing ability, were selected for the detection and analysis of the NKp30 downstream ERK pathway. WB was performed to detect the effect of B7-H6 on ERK phosphorylation. First, the expression of ERK and p-ERK was detected in NK-92 alone cells, and the p-ERK/T-ERK result was 0.10 ± 0.02 . Next, the expression of ERK and p-ERK was analyzed in NK-92 cells from the NK-92+hNC and NK-92+hB7-H6 groups following co-culture. The results of p-ERK/T-ERK were 0.32 ± 0.05 and 0.84 ± 0.10 . The p-ERK/T-ERK was significantly increased in the NK-92+hNC ($P<0.05$) and NK-92+hB7-H6 ($P<0.0001$) groups compared with that in the NK-92 alone group, with the increase in the NK-92+hB7-H6 group being more obvious. As compared with that in the NK-92+hNC group, the p-ERK/T-ERK in the NK-92+hB7-H6 group was also significantly increased ($P<0.001$; Figure S4).

5. Discussion

Cervical cancer is the leading cause of cancer death among women in developing countries [11]. At present, the clinical options for patients with persistent, recurrent and distant metastasis of cervical cancer are

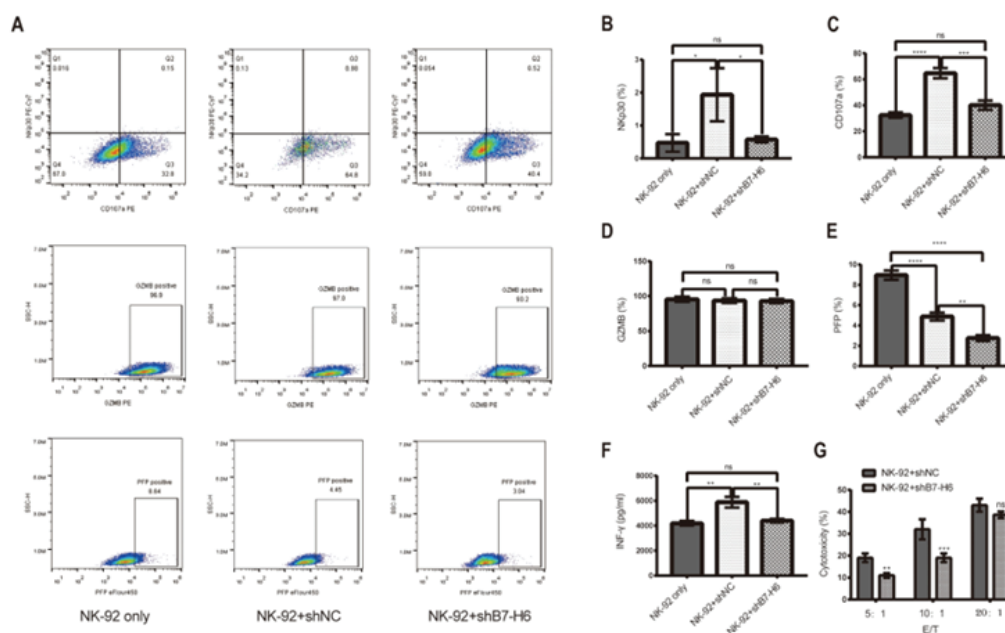


Figure S2: Effect of B7-H6 knockdown on NKp30 expression and NK cell killing function. (A) Diagram of flow detection results. (B) Following cell co-culture, the rate of NKp30+ cells in the NK-92+shB7-H6 group was no different from that in the NK-92 alone group, while that in the NK-92+shNC group was higher than that in the NK-92 alone and NK-92+shB7-H6 groups. (C) The rate of CD107a+ cells following co-culture in the NK-92+shB7-H6 groups was no different from that in the NK-92 alone group, while that in the NK-92+shNC group was higher than that in the NK-92 alone and NK-92+shB7-H6 groups. (D) In the NK-92 alone, NK-92+shNC and NK-92+shB7-H6 groups, the positive rate of NK-92 cells secreting GZMB exhibited no statistically significant difference. (E) The rate of NK-92+ cells secreting PFP in the NK-92+shNC and NK-92+shB7-H6 cells was decreased compared with that in the NK-92 alone group, while that in the NK-92+shNC group was higher than that in the NK-92+shB7-H6 group. (F) Following cell co-culture, the concentration of INF- γ secreted by NK-92 cells in the NK-92+shB7-H6 group was no different from that in the NK-92 alone group, while that in the NK-92+shNC group was higher than that in the NK-92 alone and NK-92+shB7-H6 groups. (G) The NK-92 cell killing rate in the NK-92+shB7-H6 group was lower than that in the NK-92+shNC group at an E:T of 5:1 and 10:1. No difference was observed between the NK-92+shB7-H6 and NK-92+shNC groups at an E:T of 20:1. B7-H6, B7 homolog 6; NK, natural killer GZMB, granzyme B; PFP, perforin; INF- γ , interferon gamma.

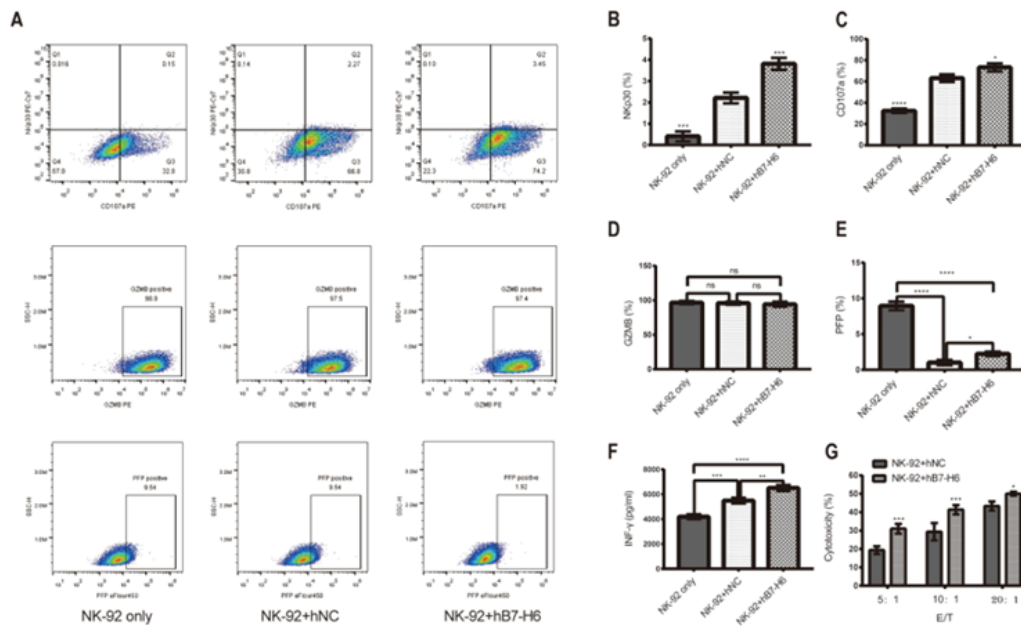


Figure S3: Effect of B7-H6 upregulation on NKp30 expression and NK cell killing function. (A) Diagram of flow detection results. (B) Following cell co-culture, the rate of NKp30+ cells in the NK-92 alone groups was lower than that in the NK-92+hNC group, and the result of NK-92+hB7-H6 was higher. (C) Following cell co-culture, the rate of CD107a+ cells in the NK-92 alone group was lower than that in the NK-92+hNC group, while that in the NK-92+hB7-H6 group was higher. (D) No statistically significant difference in the rate of NK-92+ cells secreting GZMB was observed among the NK-92 alone, NK-92+hNC and NK-92+hB7-H6 groups. (E) The rate of NK-92+ cells secreting PFP was decreased in both the NK-92+hNC and NK-92+hB7-H6 groups compared with the NK-92 alone group, while that in the NK-92+hNC group was increased compared with that in the NK-92+hB7-H6 group. (F) The concentration of INF- γ in the NK-92+hNC and NK-92+hB7-H6 groups was increased compared with that in the NK-92 alone group. The concentration of INF- γ in the NK-92+hB7-H6 group was also increased compared with that in the NK-92+hNC group. (G) The NK-92 cell killing rate in the NK-92+hB7-H6 group was increased under three different E:T compared with that in the NK-92+hNC group. B7-H6, B7 homolog 6; NK, natural killer; GZMB, granzyme B; PFP, perforin; INF- γ , interferon- γ (INF- γ).

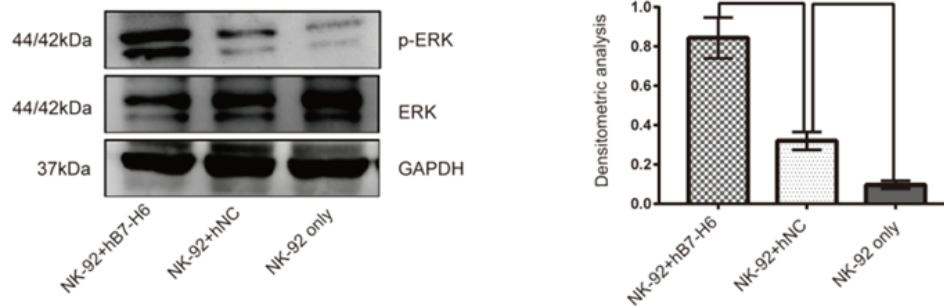


Figure S4: ERK phosphorylation in NK-92 cells following co-culture. The p-ERK/T-ERK in NK-92 cells was increased in the NK-92+hNC and NK-92+hB7-H6 groups compared with that in the NK-92 alone group, and the increase was more obvious in NK-92+hB7-H6. B7-H6, B7 homolog 6; NK, natural killer.

very limited, with only combination chemotherapy including bevacizumab, or pembrolizumab/lorlatinib/entitinib is available based on genetic test results [12], and the clinical benefits of the above treatment are not optimistic [1]. Therefore, identifying effective treatment for patients with advanced cervical cancer is urgent. The development of cervical cancer is closely associated with the imbalance between the host immune system response and tumor immune escape. Immunotherapy will become the treatment focus of advanced cervical cancer [2]. B7-H6 is a member of the B7 family. Our previous study found that B7-H6 expressed on cervical cancer cells is expected to become a new biological therapeutic target for cervical cancer [9]. Of note, however, B7-H6, also known as

NK cytotoxic receptor 3 ligand 1, can bind specifically to the active surface receptor NKp30 of NK cells through signaling motifs [13-14]. This junction plane constitutes the NKP30-B7-H6 complex [5]. NK cells are an important part of the body's innate immunity and play an important anti-infection and anti-tumor role [15]. NK cell killing status is regulated by both surface activating receptors and inhibitory receptors [16]. Activating/inhibitory receptors bind to corresponding ligands to generate activation/inhibition signals, which activate/inhibit the killing function of NK cells through a cascade of downstream signals [17]. Once activated, NK cells recruit and activate other effectors by releasing cytotoxic enzymes and soluble chemokines and inflammatory factors, including

PFp, GZMB and INF- γ at the same time [18-19]. Several studies [20-23] have shown that the specific binding of B7-H6 expressed by tumor cells with NKp30 can activate the ability of NK cells to kill tumor cells and play an important role in the anti-tumor process. In related studies on drug intervention, the positive regulation of B7-H6 on NK cell activity mediated by NKp30 was also reflected. For example, Cao et al [21] found that cisplatin and 5-fluorouracil chemotherapy, radiotherapy, non-lethal heat shock and TNF- α can induce the expression of B7-H6 in tumors, thus enhancing the sensitivity of tumors to NK cell cytotoxicity. Kellner et al [24] found that the combination of the recombinant immune ligands ULBp2:7D8 and B7-H6:7D8 can increase the NK cell-mediated killing effect in lymphoma. Of note, however, certain studies [25,26] have obtained contrasting results, suggesting that B7-H6 can lead to the immune escape of tumor cells through specific binding with NKp30, thus avoiding the protective barrier of the body's first immune defense line. The previous study found that, since the onset of cervical intraepithelial neoplasia, the expression of B7-H6 began to appear in cervical lesion tissues [9]. Therefore, it was speculated that B7-H6 not only plays a role in the progression of cervical disease, but also mediates the body's innate immunity by participating in immune regulation in cervical lesions through its special association with NKp30. In the present study, the effect of B7-H6 on NKp30 expression and NK cytotoxicity was analyzed following co-culture. The results showed that B7-H6 could promote the upregulation of NKp30 expression, increase the killing rate of NK-92 cells, and enhance the degranulation function and the secretion of INF- γ . The results of this study were similar to some recent findings suggesting that the combination of B7-H6 and NKp30 can activate the killing function of NK cells [20]. For example, Phillips et al.[22] proposed that B7-H6 can activate NK cell INF- γ secretion through NKp30, and further studied the novel synthetic peptide for tumors expressing B7-H6, which may be a promising lead for immunotherapy. PeKar et al.[23]. Found that affinity mature B7-H6 can enhance the NK cell-mediated lysis of tumor cells, and promote the release of INF- γ cytokines from bispecific immune oligomers through NKp30. Fiegler et al. [27] found that in some tumors, following the downregulation of B7-H6, NK cells' recognition ability to tumor cells was impaired. Schlecker et al.[28]. Found that, in the study of human malignant melanoma, the inhibition of B7-H6 protein hydrolysis and shedding into soluble B7-H6 can increase the expression level of B7-H6 on the surface of tumor cells, thus enhancing NKp30-mediated NK cell activation. However, the present results also suggested that the B7-H6 had no effect on the GZMB secretion capacity of NK-92 cells. What was more interesting was the detection results of PFp following cell co-culture, which suggested that the combined effect of multiple cytokines expressed by HeLa cells reduces the PFp secretion capacity, but B7-H6, as an independent influencing factor, can improve the PFp secretion capacity. The results of the present study suggested that B7-H6 participates in the immune regulation of cervical cancer, promoting the role of innate immunity in cervical cancer surveillance. However, based on the results of this experiment, the effect of B7-H6 on NKp30 is weak, and the effect on various NK cytotoxic factors is different; the reason for this and its significance need to be further analyzed. Of note, certain studies had contradictory findings. For example, Mantovani et al.[29] found that, when NK cells were co-cultured with hepatocellular carcinoma cells expressing B7-H6, NKp30 expression on the surface of NK cells was significantly decreased, with this regulatory effect eliminated following B7-H6 silencing. Pesce et al.[30]. Found that, in ovarian cancer patients, soluble B7-H6 concentration was significantly correlated with the downregulation of NKp30, which led to a decrease in the INF- γ release and cytotoxicity of NK cells, and reduced the killing of B7-H6+ ovarian cancer cells by NK cells. Ponath et al.[25]. Found that, following co-culture of isolated soluble B7-H6 with NK cells, the expression of NKp30 was downregulated, and the killing activity of NK cells decreased. Thomas et al.[26] found that, in cell lung cancer tissues and cell lines, the expression of B7-H6 exceeded that of PD-L1, and the increased expression of the B7-H6 gene was related to the decreased signal of activated natural killer cell. We speculated that B7-H6 is expressed in different tumor cells and has different regulatory effects in NK cells. NKp30 binding with the corresponding ligand can induce NK cell killing through immunoreceptor tyrosine-based activation motif [31], that is, the active receptor signal causes a series of phosphorylation reactions in NK cells. Multiple signaling cascades can occur, one of which eventually

leads to PI3K \rightarrow Rac1 \rightarrow PAK1 \rightarrow MEK \rightarrow ERK signaling cascades, thus driving the cytotoxicity of NK cells. In the present study, further analysis of ERK phosphorylation in NK-92 cells following cell co-culture showed that NKp30 upregulation and increased NK cell killing ability were accompanied by increased ERK phosphorylation. This result was consistent with the findings of Teng et al.[18] that dephosphorylation and the inactivation of ERK protein not only directly impaired NK cell killing ability, but also inhibited NK cell killing function by downregulating NKp30. These results suggested that the binding of B7-H6 with NKp30 may further affect the killing ability of NK cells by activating the downstream ERK pathway. The present study confirmed the existence of the B7-H6/NKp30 immune regulatory axis in the cervical cancer immune microenvironment, which can increase the killing effect of NK cells in cervical cancer cells. The results of this study provided insights for the research of the inherent immune regulation of cervical cancer, a new idea for the research of cervical cancer immune targets and a new molecular target for the development of cervical cancer immune drugs. However, this study had certain limitations: The cervical cancer cell line selection was too simple, and the lack of animal testing for further verification. Follow-up studies should try and overcome these limitations.

According to the present results, on the one hand, the B7-H6 expressed by cervical cancer cells can promote cervical cancer development; on the other hand, B7-H6 can also stimulate the killing effect of NK cells to cervical cancer. These opposite effects of B7-H6 on cervical cancer are noteworthy and highlight the value of B7-H6 in the study of cervical cancer. Further exploring the mechanism of B7-H6 in the development of cervical cancer will help improve the research and clinical treatment of cervical cancer.

6. Funding

Tianjin Education Commission Scientific Research Planned Project, 2022KJ252, the Tianjin Education.

References

1. Chitsike L, Duerksen-Hughes P. The Potential of Immune Checkpoint Blockade in Cervical Cancer: Can Combinatorial Regimens Maximize Response? A Review of the Literature. *Curr Treat Options Oncol.* 2020; 21(12): 95.
2. Zhu SY, Wu QY, Zhang CX, Wang Q, Ling J. miR-20a inhibits the killing effect of natural killer cells to cervical cancer cells by downregulating RUNX1. *BiochemBiophys Res Commun.* 2018; 505(1): 309-316.
3. David BA, Jane MC and Marco C: The Natural Cytotoxicity Receptors in Health and Disease. *Front Immunol.* 2019; 909-930.
4. Ni L, Dong C: New B7 Family Checkpoints in Human Cancers. *Mol Cancer Ther.* 2017; 16(7): 1203-1211.
5. Li Y, Mariuzza RA. Structural basis for recognition of cellular and viral ligands by NK cell receptors *Front Immunol.* 2014; 123-143.
6. Li Y, Wang Q and Mariuzza RA. Structure of the human activating natural cytotoxicity receptor NKp30 bound to its tumor cell ligand B7-H6. *J Exp Med.* 2011; 208(4): 703-714.
7. Joyce MG, Tran P, Zhuravleva MA, Jaw J. Crystal structure of human natural cytotoxicity receptor NKp30 and identification of its ligand binding site. *Proceedings of the National Academy of Sciences of the United States of America.* 2011; 108(15): 6223-6228.
8. Textor S, Bossler F, Henrich KO. The proto-oncogene Myc drives expression of the NK cell-activating NKp30 ligand B7-H6 in tumor cells. *Oncoimmunology.* 2016; 5(7): e1116674.
9. Guo R, Liu G, Li C. B7 homolog 6 promotes the progression of cervical cancer. *Exp Ther Med.* 2021; 22(1): 774.
10. Liu X, Guo R, Xu Y. B7-H6 as a Diagnostic Biomarker for Cervical Squamous Cell Carcinoma. *Genet Test Mol Biomarkers.* 2021; 25(7): 463-470.
11. Stelzle D, Tanaka LF, Lee KK. Estimates of the global burden of cervical cancer associated with HIV. *Lancet Glob Health.* 2021; 9(2): e161-e169.
12. Abu-Rustum NR, Yashar CM, Bradley K. NCCN Guidelines Version 1. 2021 Cervical Cancer. 2021.

13. Chen Y, Mo J, Jia X, He Y. The B7 Family Member B7-H6: a New Bane of Tumor. *Pathol Oncol Res.* 2018; 24(4): 717-721.
14. Skořepa O, Pazický S, Kalousková B. Natural Killer Cell Activation Receptor NKp30 Oligomerization Depends on Its N-Glycosylation. *Cancers (Basel).* 2020; 12(7).
15. Sivori S, Vacca P, Del Zotto G, Munari E, Mingari MC, Moretta L. Human NK cells: surface receptors, inhibitory checkpoints, and translational applications. *Cell Mol Immunol.* 2019; 16(5): 430-441.
16. Pinheiro PF, Justino GC, Marques MM. NKp30 - A prospective target for new cancer immunotherapy strategies. *Br J Pharmacol.* 2020; 177(20): 4563-4580.
17. Myers JA, Miller JS. Exploring the NK cell platform for cancer immunotherapy. *Nat Rev Clin Oncol.* 2021; 18(2): 85-100.
18. Teng R, Wang Y, Lv N. Hypoxia Impairs NK Cell Cytotoxicity through SHP-1-Mediated Attenuation of STAT3 and ERK Signaling Pathways. *J Immunol Res.* 2020; 4598476.
19. Barrow AD, Martin CJ, Colonna M. The Natural Cytotoxicity Receptors in Health and Disease. *Front Immunol.* 2019; 10: 909.
20. Hu Y, Zeng T, Xiao Z. Immunological role and underlying mechanisms of B7-H6 in tumorigenesis. *Clin Chim Acta.* 2020; 502: 191-198.
21. Guoshuai C, Jian W, Xiaodong Z, Haiming W, Zhigang T, Rui S. Tumor Therapeutics Work as Stress Inducers to Enhance Tumor Sensitivity to Natural Killer (NK) Cell Cytolysis by Up-regulating NKp30 Ligand B7-H6. *J Biol Chem.* 2015; 290(50).
22. Phillips M, Romeo F, Bitsaktis C, Sabatino D. B7H6-derived peptides trigger TNF- α -dependent immunostimulatory activity of lymphocytic NK92-MI cells. *Biopolymers.* 2016; 106(5): 658-72.
23. Pekar L, Klausz K, Busch M. Affinity Maturation of B7-H6 Translates into Enhanced NK Cell-Mediated Tumor Cell Lysis and Improved ProInflammatory Cytokine Release of Bispecific Immunoligands via NKp30 Engagement. *J Immunol.* 2021; 206(1): 225-236.
24. Kellner C, Günther A, Humpe A. Enhancing natural killer cell-mediated lysis of lymphoma cells by combining therapeutic antibodies with CD20-specific immunoligands engaging NKG2D or NKp30. *Oncoimmunology.* 2016. 5(1): e1058459.
25. Ponath V, Hoffmann N, Bergmann L. Secreted Ligands of the NK Cell Receptor NKp30: B7-H6 Is in Contrast to BAG6 Only Marginally Released via Extracellular Vesicles. *Int J Mol Sci.* 2021; 22(4).
26. Thomas PL, Groves SM, Zhang YK. Beyond Programmed Death-Ligand 1: B7-H6 Emerges as a Potential Immunotherapy Target in SCLC. *J Thorac Oncol.* 2021.
27. Fiegler N, Textor S, Arnold A. Downregulation of the activating NKp30 ligand B7-H6 by HDAC inhibitors impairs tumor cell recognition by NK cells. *Blood.* 2013; 122(5): 684-93.
28. Schlecker E, Fiegler N, Arnold A. Metalloprotease-mediated tumor cell shedding of B7-H6, the ligand of the natural killer cell-activating receptor NKp30. *Cancer Res.* 2014; 74(13): 3429-40.
29. Mantovani S, Oliviero B, Lombardi A. Deficient Natural Killer Cell NKp30-Mediated Function and Altered NCR3 Splice Variants in Hepatocellular Carcinoma. *Hepatology.* 2019; 69(3): 1165-1179.
30. Pesce S, Tabellini G, Cantoni C, Patrizi O, Coltrini D. B7-H6-mediated downregulation of NKp30 in NK cells contributes to ovarian carcinoma immune escape. *Oncoimmunology.* 2015; 4(4): e1001224.
31. Meza Guzman LG, Keating N, Nicholson SE. Natural Killer Cells: Tumor Surveillance and Signaling. *Cancers (Basel).* 2020; 12(4).